

INCREMENTAL NONLINEAR DYNAMIC CONTROL WITH SPARSE NON-PARAMETRIC BAYESIAN REGRESSION OF DAMAGED AIRCRAFT

Lamsu Kim¹, Dongwoo Lee² & Hyochoong Bang³

^{1,2,3}Korea Advanced Institute of Science and Technology

Abstract

Unlike ground vehicles, fixed-wing aircraft that experiences structural damage faces more dangerous situations, even resulting in crash landing. Especially when the control law of the aircraft is based on the prior system model knowledge of the aircraft, it can encounter loss of control when damage is inflicted to the aircraft because the structural damage changes the parameters in the system model and control effectiveness matrix, causing divergence of the closed-loop system. This structural damage causes the aircraft to change its mass, center of gravity (CG), moment of inertia (MOI), aerodynamic coefficients and these problems impose challenges to control design as it must handle high uncertainties in the system and control effectiveness matrix. Two major approaches to deal with uncertainties are to use robust controller and estimate uncertainties which are calculated online to counter them. For this problem, we present an Incremental Nonlinear Dynamic Inversion (INDI) Control with Sparse on-line Gaussian Regression (SGPR) for controlling damaged aircraft. Incremental Dynamics are used to overcome disturbances in the system by using state derivative measurements. We applied Nonlinear Dynamic Inversion control with this Incremental Dynamics to profit from the robustness properties of this form. In addition to this control law, uncertainties are estimated using SGPR to add adaptiveness to the system; a non-parametric regression method. There are various situations of structural damage. In this study, severed single main wing tip situation is considered.

Keywords: Damaged Aircraft, Incremental Dynamics, Nonlinear Dynamic Inversion, Sparse Gaussian Process Regression

1. General Introduction

When everything is nominal, aircraft system control using perfect model-based control law does not cause any problem throughout the flight but flight in a nominal environment is but an ideal dream. Structural damage is one of many situations that induce disturbances and alter the system model and control effectiveness matrix. Structural damage in flight is uncommon in the aviation industry but does occur and must be dealt with because it leads to degradation of control performance and loss of control in the worst case. In 2003, DHL Airbus A300-B4 cargo aircraft encountered a loss of hydraulics after being hit by a missile but the crew successfully landed the plane at Baghdad International airport using asymmetric thrust control [6]. This shows that structurally damaged aircraft may still be controllable. Hence it is a paramount objective to design control law that can counter uncertainties due to structural damage. In this paper, the design of control law for fixed-wing aircraft with structural damage is of interest. The model used is a reduced-order model (ROM) of generic transport model (GTM) presented in [9]. As for the damage, a severed left-wing case is considered only.

The mass, MOI, the CG, and aerodynamic coefficients are the four main properties that change when damage is inflicted on the aircraft. The aircraft is almost symmetric along the xy and yz plane of the

body-fixed frame, thus coupled MOI I_{xy} and I_{yz} are negligible. When damage occurs, these values are no longer negligible and the dynamics of the aircraft change causing unwanted moments. The CG also shifts after damage. Since sensors are attached to an aircraft reference frame that is fixed closely at the CG point initially, a shift in CG due to damage will create additional force and moment terms. All these additional moments and forces must be compensated using a controller. The dynamics equation when the MOI changes and CG shifts from a fixed reference point other than the CG point with non-zero elements inertia matrix must be derived to examine the motion and design controller, which will be explained in section 2. Aerodynamic coefficients also change because the shape of the aircraft is reconfigured after damage. Since it is hard to obtain aerodynamic coefficients for all damaged scenarios, it is efficient to estimate uncertainties arising from aerodynamic uncertainties online. To control fixed-wing aircraft under these uncertainties, we present an Incremental Nonlinear Dynamic (INDI) Control with Sparse Gaussian Regression (SGPR) of the damaged aircraft. Though there are various situations of structural damage, we considered severed single main wing tip situation only.

Recent studies include linear controllers and nonlinear controllers for fixed-wing aircraft under normal or disturbance and uncertainties induced situations. The linear controllers use linearized plant dynamics at different sets of states and apply linear control methods like Linear Quadratic Regulator(LQR), H_∞ and Proportional Integral Derivative (PID) control. When an aircraft is damaged, the dynamics equation changes significantly, and pre-determined linearized plant dynamics used for the control design differ a lot from the nominal system. The robust linear controllers are studied and developed to cope with this problem but they require knowledge of the bound of uncertainties which are burdensome tasks to find. It is not efficient to choose large uncertainties bounds to alleviate works on finding bounds since it will lead to large tracking error performances [5]. Let alone finding the bounds of the uncertainties, designing linear controllers for all linearized plants is also a tedious work. The nonlinear controllers like Nonlinear Dynamic Inversion(NDI) and Backstepping are free from this problem but they face the same problem of performance degradation from damage since they also use *a priori* system models and control effectiveness matrix. When the difference between the dynamics model to the true damaged system is not negligible, a closed-loop system with these nonlinear controllers may also become unstable. The sliding Mode Controllers (SMC) method can add robustness to the nonlinear controller but it have inherent chattering problem.

Among these control laws, the Nonlinear Dynamic Inversion control (NDI) is a widely used control scheme in the military [2]. The NDI control law uses linear control law on the linearized system model that was not obtained using a numerical linearization method like the Taylor series expansion. The linearization uses a diffeomorphic mapping function to map the state space of the nominal nonlinear system to a linearized system. The mapping function guarantees the diffeomorphism when the system knowledge of the true system is exact. The apparent disadvantage of the NDI control law is that the performance of the controller degenerates when uncertainties increases [11]. To mitigate the reliance on the system model and uncertainties, the INDI law was proposed. INDI controller is a sensor-based control that uses incremental dynamics and linear control law. The incremental dynamics is derived using the assumptions that the sample time is small, and the change in the control input affects the state derivative considerably larger than the change in the system states. With state derivative measurements and assumptions, the INDI is known to have robustness to uncertainties. The magnitude of the disturbance terms decreases as the sampling time decreases [12]. This means that INDI is less susceptible to changes in the system model compared to the NDI control law and is dependent on the control effectiveness matrix due to these assumptions.

In this paper, the control of the pre-mentioned damaged fixed-wing aircraft is designed using INDI control as a baseline controller for robustness and SGPR for adaptiveness. The sample time is normally determined by the performance of the flight control computer (FCC) and is fixed and does not change throughout the flight after FCC is determined, hence robustness of the system cannot be tuned easily. Also, the performance may degrade when upset to state derivative due to change in

state variable is no longer negligible and the uncertainties in the control effectiveness matrix \mathbf{B} increase. For these reasons, we provided adaptiveness to the control law using SGPR. The uncertain terms are easily estimated when their parametric basis functions are known but they are very hard to know. Also using a parametric basis function can overfit the controller to certain situations only. It is ideal to use regression methods with non-parametric basis functions, meaning infinitely many parameters, for general purposes and SGPR is one of them. So, we applied SGPR to estimate the uncertainties due to structural damage. In this way, we aimed to benefit from the adaptiveness of SGPR, and the robustness properties of the incremental dynamics.

The paper is structured as follows. This section 1 explains the general introduction. Section 2 derives the equation of motion of an arbitrary point on a rigid body, offset from the CG. Section 3 explains the ROM. The base-line controller are explained in section 4. where SGPR in section 5. Section 6 shows the simulation results. Conclusions are presented in section 7.

2. Equations of Motion Centered at an Arbitrary Point on a Rigid Body

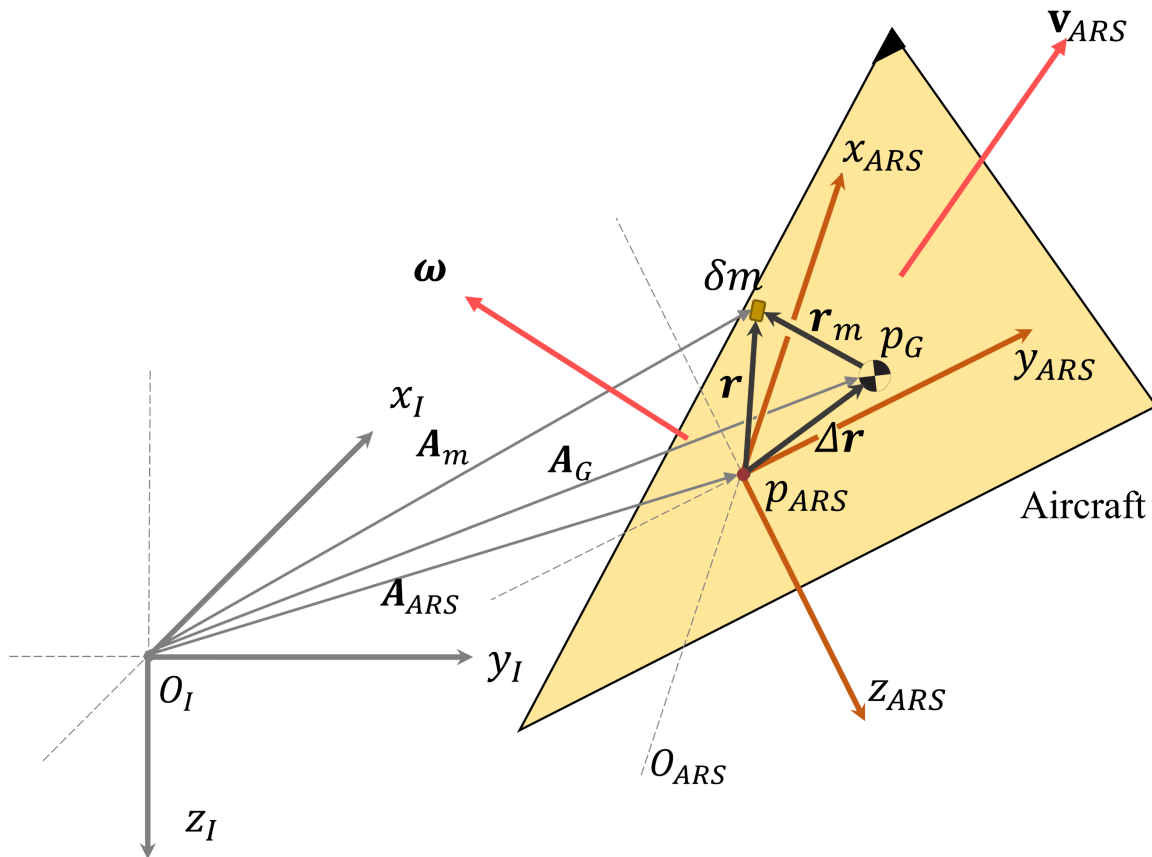


Figure 1 – Arbitrary body frame on a fixed point relative to inertial and CG centered body frame

Normally, the equation of motion for aircraft is derived without considering CG shift since it is a reasonable assumption that the CG point does not change during flight. This is hardly the case for aircraft with damage. Sensors are attached to the Aircraft Reference System (O_{ARS}) frame. Initially, this frame is closely centered at the CG point. If the CG point does not shift during the flight, sensor measurements are assumed to have close values to that of the CG point. The damage to the aircraft cause shift in CG and offset between the O_{ARS} frame and CG point gets larger, creating additional force and moment acting on O_{ARS} frame. In this case, effect from CG shift is no longer insignificant. The derivation of the general equation of motion of O_{ARS} frame with arbitrary CG shift can be derived using Newton's law as below.

Referring to figure 1, the relative distance \mathbf{r} from p_{ARS} to elemental mass δm is

$$\mathbf{r} = \mathbf{r}_m + \Delta \mathbf{r} \quad (1)$$

where $\Delta \mathbf{r} = [\Delta x, \Delta y, \Delta z]$ is offset vector from p_{ARS} to shifted CG point p_G . Using Newton's Law of motion, the external force \mathbf{F}_B in the inertial frame O_I is equal to adding all linear momentum of the δm

$$\mathbf{F}_B = \sum \delta \mathbf{F}_B = \sum \left(\frac{d}{dt} \left(\mathbf{v}_{ARS} + \frac{d\mathbf{r}}{dt} \right) \right)_I \delta m \quad (2)$$

where $\mathbf{v}_{ARS} = [u, v, w]$ is the body linear velocity in O_{ARS} , $\boldsymbol{\omega} = [p, q, r]$ is the body rate also in O_{ARS} . Both vector sum undergoes the time derivative in the inertial frame O_I . Simplifying,

$$\mathbf{F}_B = m \frac{d}{dt} (\mathbf{v}_{ARS} + \boldsymbol{\omega} \times \mathbf{r})_I \quad (3)$$

The subscript I denotes that the derivative is done on I frame. m is the total mass. Applying transport theorem and neglecting the term from time rate of change in CG location,

$$\mathbf{F}_B = m \dot{\mathbf{v}}_{ARS} + m \dot{\boldsymbol{\omega}} \times \Delta \mathbf{r} + m \boldsymbol{\omega} \times (\mathbf{v}_{ARS} + \boldsymbol{\omega} \times \Delta \mathbf{r}) \quad (4)$$

where $\dot{\mathbf{v}}_{ARS} = [\dot{u}, \dot{v}, \dot{w}]$ and $\dot{\boldsymbol{\omega}} = [\dot{p}, \dot{q}, \dot{r}]$. the $\dot{\bullet}$ accent denotes time derivative of variable \bullet on the frame O_{ARS} .

The angular moment equation is derived in similar manner. The angular momentum \mathbf{H}_B at point p_{ARS} is,

$$\mathbf{H}_B = \int (\mathbf{r} \times (\mathbf{v}_{ARS} + \boldsymbol{\omega} \times \mathbf{r})) \delta m \quad (5)$$

Then the equation becomes,

$$\mathbf{H}_B = \mathbf{I} \boldsymbol{\omega} + m \Delta \mathbf{r} \times \mathbf{v}_{ARS} \quad (6)$$

where \mathbf{I} is the MOI matrix. The time derivative of the angular momentum in O_{ARS} frame becomes

$$\begin{aligned} \frac{d}{dt} (\mathbf{H}_B)_I &= \int \left(\frac{d}{dt} (\mathbf{r})_I \times \mathbf{v}_{\delta m} \right) \delta m + \int \left(\mathbf{r} \times \frac{d}{dt} (\mathbf{v}_{\delta m})_I \right) \delta m \\ &= \int \left(\left(\frac{d}{dt} (\mathbf{A}_{\delta m})_I - \frac{d}{dt} (\mathbf{A}_{ARS})_I \right) \times \mathbf{v}_{\delta m} \right) \delta m + \mathbf{M}_B \end{aligned} \quad (7)$$

where the external moment on the inertial frame $\mathbf{M}_B = \int (\mathbf{r} \times \frac{d}{dt} (\mathbf{v}_{\delta m})_I) \delta m$ by definition. Since $\frac{d}{dt} (\mathbf{A}_{\delta m})_I = \mathbf{v}_{\delta m}$ and $\frac{d}{dt} (\mathbf{A}_{ARS})_I = \mathbf{v}_{ARS}$, they become

$$\begin{aligned} \mathbf{M}_B &= \frac{d}{dt} (\mathbf{H}_B)_I + m \mathbf{v}_{ARS} \times (\mathbf{v}_{ARS} + (\dot{\Delta \mathbf{r}})_I) \\ &= \frac{d}{dt} (\mathbf{H}_B)_I + m \boldsymbol{\omega} \times \Delta \mathbf{r} \end{aligned} \quad (8)$$

Finally, the moment equation is obtained as,

$$\mathbf{M}_B = \mathbf{I} \dot{\boldsymbol{\omega}} + m \Delta \mathbf{r} \times \dot{\mathbf{v}}_{ARS} + \boldsymbol{\omega} \times \mathbf{I} \boldsymbol{\omega} + m \boldsymbol{\omega} \times (\Delta \mathbf{r} \times \mathbf{v}_{ARS}) + m \mathbf{v}_{ARS} \times (\boldsymbol{\omega} \times \Delta \mathbf{r}) \quad (9)$$

The above equations can be simplified in matrix form as organized from [1]

$$\begin{bmatrix} \dot{\mathbf{v}}_{ARS} \\ \dot{\boldsymbol{\omega}} \end{bmatrix} = \begin{bmatrix} m \mathbf{I}_{3 \times 3} & -\mathbf{M} \\ \boldsymbol{\Omega}_D & \mathbf{I} \end{bmatrix}^{-1} \left(\begin{bmatrix} \mathbf{F}_B \\ \mathbf{M}_B \end{bmatrix} - \begin{bmatrix} m \boldsymbol{\Omega}_D & -\boldsymbol{\Omega}_D \mathbf{M} \\ \boldsymbol{\Omega}_D \mathbf{M} & \boldsymbol{\Omega}_D \mathbf{I} - \mathbf{V}_D \mathbf{M} \end{bmatrix} \begin{bmatrix} \mathbf{v}_{ARS} \\ \boldsymbol{\omega} \end{bmatrix} \right) \quad (10)$$

where

$$\begin{aligned} \mathbf{M} &= \begin{bmatrix} 0 & -m \Delta z & m \Delta y \\ m \Delta z & 0 & -m \Delta x \\ -m \Delta y & m \Delta x & 0 \end{bmatrix}, \boldsymbol{\Omega}_D = \begin{bmatrix} 0 & -r & q \\ r & 0 & -p \\ -q & p & 0 \end{bmatrix} \\ \mathbf{V}_D &= \begin{bmatrix} 0 & -w & v \\ w & 0 & -u \\ -v & u & 0 \end{bmatrix}, \mathbf{I} = \begin{bmatrix} I_{xx} & -I_{xy} & -I_{xz} \\ -I_{xy} & I_{yy} & -I_{yz} \\ -I_{xz} & -I_{yz} & I_{zz} \end{bmatrix} \end{aligned} \quad (11)$$

3. Reduced Order Model

The damaged aircraft model used is the GTM. This GTM is a 5.5% scaled model of a commercial jet airliner developed by NASA to obtain changes in the aerodynamic coefficients, mass and inertia properties, and CG. There were various attempts made to analyze this damaged model. The wind tunnel test on this model was performed in [10]. The assessment concerning the stability derivatives changes of the GTM model was performed in [7]. In [9], effects on structural load were explored on the damaged main wing of the GTM and derived the ROM for the nominal and damaged GTM. In this paper, we simulated the damaged aircraft model using this ROM model used in [9] and applied our proposed control law.

3.1 Aerodynamic Coefficients of normal and damaged GTM

State	longitudinal			lateral		
	C _D	C _L	C _m	C _Y	C _l	C _n
0	0.0279	0.0327	0.1569	0	0	0
α	0	5.9419	-1.8641	0	0	0
α^2	2.0137	-0.2031	-0.6088	0	0	0
\bar{q}	0.4373	16.000	-54.1055	0	0	0
\bar{q}^2	-59.8215	-0.2884	-9.4867	0	0	0
δ_e	0	1.1267	-4.2718	0	0	0
δ_e^2	1.2721	0.0343	0	0	0	0
β	0	0	0	-0.8281	-0.1504	0.2153
β^2	-0.6123	0.1349	-1.7395	0	0	0
\bar{q}	0	0	0	-0.2159	-0.4420	0.0465
\bar{q}^2	-0.5697	0.0390	-0.2241	0	0	0
\bar{r}	0	0	0	0.6451	0.1285	-0.4227
\bar{r}^2	-0.4101	0.0774	-1.3550	0	0	0
δ_a	0	0	0	0.0143	0.0949	0
δ_a^2	0.0434	-0.0008	0.0122	0	0	0
δ_r	0	0	0	-0.4990	-0.0664	0.2269
δ_r^2	0.1803	-0.1395	0.6026	0	0	0

Table 1 – ROM Aerodynamic Coefficients of GTM with no Damage [9]

Table 1 shows the aerodynamic coefficients of the ROM for GTM in nominal condition. In the table, α and β are angle of attack and side-slip angle, $\bar{p} = \frac{\bar{c}p}{2Vt}$, $\bar{q} = \frac{bq}{2Vt}$, $\bar{r} = \frac{\bar{c}r}{2Vt}$ is the normalized roll, pitch, yaw rate where \bar{c} , b , Vt are the chord length, span and true air speed of the aircraft. δ_e , δ_a and δ_r are the deflection of the elevator, aileron, and ruder control surfaces.

The aerodynamic coefficient of the ROM of the GTM with 33 % damaged left main wing is on the table 2. If you compare the aerodynamic coefficients of the nominal GTM model to the 33 % damaged left-wing one, you can notice that the longitudinal and lateral coefficients terms are created when the wing is severed. It is obvious since the symmetry will be violated when a portion of the left main is removed. The damage will create unwanted aerodynamic coupling force and moment. The aerodynamic coefficients in the control surfaces are also changed, hence uncertainties will add up to the nominal control effectiveness matrix **B**.

The change in aerodynamic coefficients using the table 1 and 2 are shown in figure 2 and 3. The aerodynamic coefficients variation due to left main wing tip loss versus angle of attack is shown in figure 2 with zero actuator deflection angle. The change in aerodynamic coefficients of actuators versus wing loss in percentage is shown in figure 3. For brevity, only the moment aerodynamic coefficients are displayed in the figures.

State	longitudinal			lateral		
	C _D	C _L	C _m	C _Y	C _l	C _n
0	0.0275	0.0186	0.1673	-0.0006	-0.0042	0.0001
α	0	5.1308	-1.3938	-0.0300	-0.2446	-0.0092
α^2	1.7468	-0.1972	-0.5371	0.2334	0.0137	-0.1981
\bar{q}	0.4621	14.9681	-53.4648	-0.0386	-0.3218	-0.0160
\bar{q}^2	-58.6255	0.2680	-9.8754	0.5280	0.1581	-0.4000
δ_e	0	1.1192	-4.2686	-0.0001	-0.0023	-0.0002
δ_e^2	1.2777	0.0344	0	0.0002	0	-0.0004
β	-0.0003	0.0536	-0.0332	-0.8253	-0.1329	0.2160
β^2	-0.6118	0.1409	-1.7475	0	0	0
\bar{q}	-0.0066	0.4644	-0.2741	-0.1989	-0.2980	0.0531
\bar{q}^2	-0.3719	0.0368	-0.1974	0.1221	-0.0005	-0.0973
\bar{r}	-0.0011	-0.0244	0.0157	0.6435	0.1199	-0.4225
\bar{r}^2	-0.4108	0.0674	-1.3499	0	-0.0045	0
δ_a	-0.0012	-0.1345	0.1067	0.0072	0.0478	0
δ_a^2	0.0216	-0.0004	0.0061	-0.0045	0	0.0099
δ_r	0	-0.0009	0	-0.4989	-0.0666	0.2268
δ_r^2	0.1803	-0.1395	0.0625	0	0	0

Table 2 – ROM Aerodynamic Coefficients of GTM with 33 % Severed Left Wing [9]

3.2 Mass Properties of normal and damaged GTM

The damage on the left main wing tip does not affect only the aerodynamic coefficients of the aircraft but also the mass properties like mass, the MOI, and the location of the CG. The variation of the mass, MOI, and CG shift is displayed in figure 4. These data is attained from [8]. Among those mass properties, CG shift creates the most unexpected force and moments on the body as was shown in the equation derived in section 2. that could easily have been disregarded when mass and MOI change were only considered to simulate damaged fixed-wing aircraft.

4. Incremental Nonlinear Dynamics Inversion Control

The performance of the traditional NDI control depends heavily on the *a priori* knowledge of the system. The performance of any model-based control law relies on the accuracy of model knowledge. Though the system knowledge is perfectly known, if the dynamics changes during operation by chance, the performance degradation occurs; in the worst case, the system falls into inoperable condition. To mitigate this dependency issue on the model accuracy, incremental dynamics were formulated and used for control law derivation.

4.1 Incremental Nonlinear Dynamics

The derivation of INDI is as follows. Given the state derivative equation of the system as

$$\dot{\mathbf{x}} = \mathbf{f}(\mathbf{x}, \mathbf{u}) \quad (12)$$

where \mathbf{x} is a state column vector, \mathbf{u} is a control input vector. Applying Taylor series expansion to the above equation, it becomes

$$\dot{\mathbf{x}} \approx \mathbf{f}(\mathbf{x}_0, \mathbf{u}_0) + \frac{\partial \mathbf{f}}{\partial \mathbf{x}}(\mathbf{x} - \mathbf{x}_0) + \frac{\partial \mathbf{f}}{\partial \mathbf{u}}(\mathbf{u} - \mathbf{u}_0) \quad (13)$$

where subscript '0' means the most recent value. Re-writing the above equation becomes

$$\begin{aligned} \dot{\mathbf{x}} &\approx \dot{\mathbf{x}}_0 + \mathbf{F}(\mathbf{x} - \mathbf{x}_0) + \mathbf{B}(\mathbf{u} - \mathbf{u}_0) \\ \dot{\mathbf{x}} &\approx \dot{\mathbf{x}}_0 + \mathbf{B}(\mathbf{u} - \mathbf{u}_0) \end{aligned} \quad (14)$$

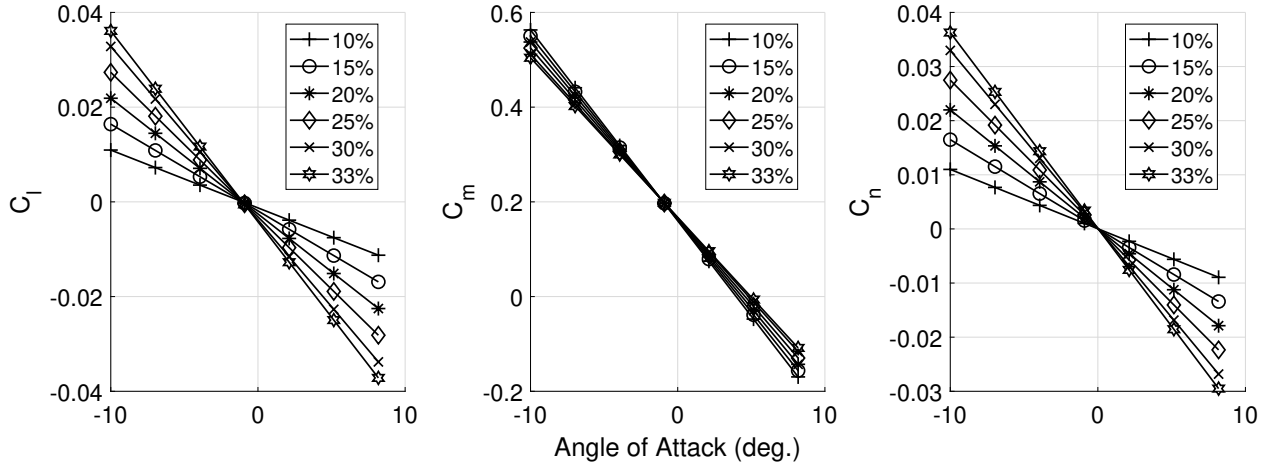


Figure 2 – Change in Roll, Pitch and Yaw Moment Aerodynamic Coefficients VS Angle of Attack from Left Main Wing Loss

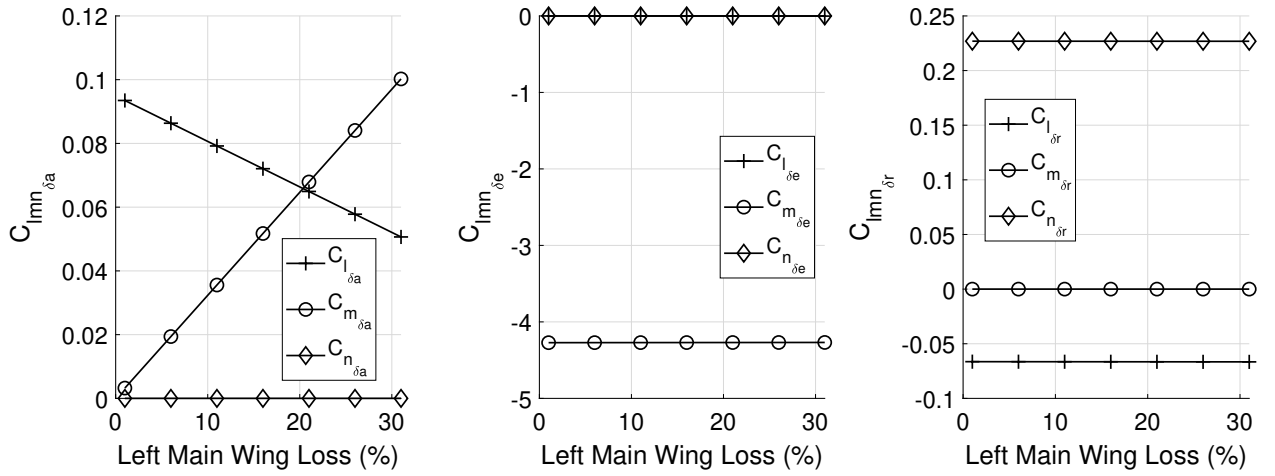


Figure 3 – Change in Roll, Pitch and Yaw of Actuator Moment Aerodynamic Coefficients V.S. Percentage of Left Main Wing Loss

This equation 14 is called the incremental dynamics. The INDI control law assumes that the $\mathbf{x} \approx \mathbf{x}_0$ and $\mathbf{u} \neq \mathbf{u}_0$ due to the assumptions as stated above and cancels the $\mathbf{F}(\mathbf{x} - \mathbf{x}_0)$ from the equation. With this incremental nonlinear dynamics equation, the control law and virtual input $\mathbf{v} \approx \dot{\mathbf{x}}$, the control input is obtained as

$$\begin{aligned} \dot{\mathbf{x}} &\approx \dot{\mathbf{x}}_0 + \mathbf{B}(\mathbf{u} - \mathbf{u}_0) \\ \mathbf{u} &= \mathbf{u}_0 + \mathbf{B}^{-1}(\mathbf{v} - \dot{\mathbf{x}}_0) \end{aligned} \quad (15)$$

Although INDI has robustness compared to NDI, to gain more robustness to large uncertainties like in this damaged aircraft situation (change in mass, CG location, MOI, and aerodynamic coefficients), uncertain parameters must be estimated to compensate its effect. In [11], the uncertainties in the control effectiveness matrix \mathbf{B} can affect the performance of the INDI controller compared to model uncertainties \mathbf{F} . Also, the INDI controller can lose its robustness when the assumption that the change in control inputs governs the magnitude of the state derivatives equation no longer holds, creating dependency in \mathbf{F} and state $\mathbf{x} - \mathbf{x}_0$. If the uncertainties in the model and control effectiveness matrix increase due to structural damage and effect of \mathbf{F} is no longer negligible, then the INDI controller may experience performance degradation or fall into instability. This means that if these uncertainties are estimated, used as feedforward terms in the controller, and cancelled, controller can have adaptiveness together with the inherent robustness that the INDI has. For this purpose, SGPR is used, which is explained in section 5.

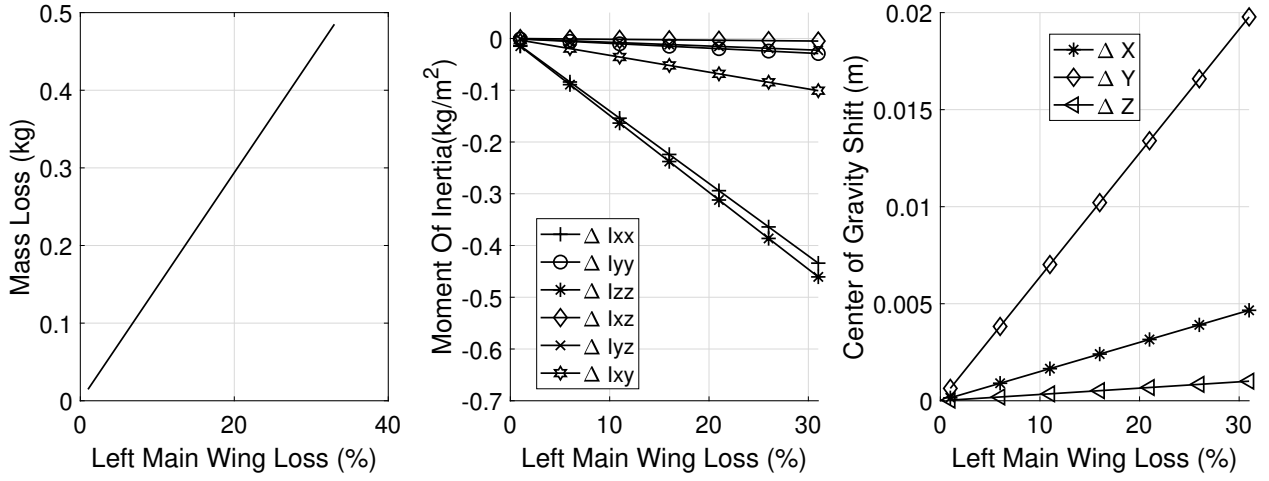


Figure 4 – Change in Mass Properties from Left Main Wing Loss [8]

4.2 Control using Incremental Nonlinear Dynamics

The control law is derived using INDI for the damaged aircraft case when no damage is incurred. Due to equation 11, the equation 14 becomes

$$\dot{\mathbf{x}} = \dot{\mathbf{x}}_0 + (\hat{\mathbf{F}} + \delta\mathbf{F})(\mathbf{x} - \mathbf{x}_0) + (\hat{\mathbf{B}} + \delta\mathbf{B})(\mathbf{u} - \mathbf{u}_0) + \mathbf{d} \quad (16)$$

where $\mathbf{F} = (\hat{\mathbf{F}} + \Delta\mathbf{F})$, $\mathbf{B} = (\hat{\mathbf{B}} + \Delta\mathbf{B})$ and \mathbf{d} is disturbance term. The $\hat{\mathbf{F}}$ and $\hat{\mathbf{B}}$ are the *a priori* information about \mathbf{F} and \mathbf{B} , $\Delta\mathbf{F}$ and $\Delta\mathbf{B}$ are the uncertainties created due to damage. After applying the following control input to equation 15

$$\mathbf{u} = \mathbf{u}_0 + \hat{\mathbf{B}}^{-1}(\mathbf{v} - \dot{\mathbf{x}}_0) \quad (17)$$

the equation 16 becomes,

$$\begin{aligned} \dot{\mathbf{x}} &= \mathbf{v} + \Delta \\ \Delta &= \delta\mathbf{F}(\mathbf{x} - \mathbf{x}_0) + \delta\mathbf{B}(\mathbf{u} - \mathbf{u}_0) + \mathbf{d} \end{aligned} \quad (18)$$

Selecting pseudo control input \mathbf{v} as

$$\mathbf{v} = \mathbf{v}_c - \mathbf{v}_\Delta \quad (19)$$

where \mathbf{v}_c is the user chosen control input. If the uncertainty Δ is estimated such that $\mathbf{v}_\Delta \approx \Delta$, the equation 18 becomes

$$\dot{\mathbf{x}} \approx \mathbf{v}_c \quad (20)$$

5. Uncertainties Estimation

The ordinary model-based controller may work fine for GTM under nominal conditions. After the model experiences damage, the system dynamics and control effective matrix change, causing abnormal behavior compared to the expected control response. The INDI uses Taylor series expansion when obtaining the incremental dynamics, so the basis functions for this dynamics are hard to be formulated. If this was possible, parametric functions could have been used and various adaptive control methods can be applied. The basis functions for additional disturbances are also hard to find. For estimation of these changes, we used SGPR which is a non-parametric GP model with sparsity consideration.

5.1 Gaussian Process Regression

A stochastic process is a process composed of random variables indexed with spatial or temporal components. A Gaussian Process (GP) is a type of stochastic process where the random variables follows Multivariate Normal distribution. The GP regression uses Bayesian inference with GP priors to estimate posterior given the dataset $\mathbf{D} = [(y_{t=0}, \mathbf{x}_{t=0}), (y_{t=1}, \mathbf{x}_{t=1}), \dots, (y_{t=N}, \mathbf{x}_{t=N})]$ with measurement vector y , input state \mathbf{x} , and time index \mathbf{t} . From [13], the function $\mathbf{f}(\mathbf{x})$ is defined as

$$\begin{aligned} \mathbf{f}(\mathbf{x}) &\sim \mathbf{GP}(m(\mathbf{x}), k(\mathbf{x}, \mathbf{x}')) \\ m(\mathbf{x}) &= \mathbb{E}[f(\mathbf{x})] \\ k(\mathbf{x}, \mathbf{x}') &= \mathbb{E}[(f(\mathbf{x}) - m(\mathbf{x}))(f(\mathbf{x}') - m(\mathbf{x}'))] \end{aligned} \quad (21)$$

where $m(\mathbf{x})$ is the mean and $k(\cdot, \cdot)$ kernel function. There are many candidate functions for kernel $k(\cdot, \cdot)$. In this research, the exponential kernel is used, which is the most general one. The exponential kernel is,

$$k(x, x') = \exp\left(-\frac{\|x - x'\|^2}{2\sigma_x^2}\right) \quad (22)$$

Typical the uncertainties $\Delta = f(\mathbf{x}_i)$ are composed of unknown functions whose number of basis functions are also not known. The measurement of Δ is y_i that includes the noise w as

$$\begin{aligned} y_i &= f(\mathbf{x}_i) + w_i \\ w_i &\sim N(0, \sigma_i^2) \end{aligned} \quad (23)$$

The uncertainties Δ can be estimated using GP Regression as

$$\begin{bmatrix} \mathbf{y}_t \\ y_{t+1} \end{bmatrix} \sim N\left(\mathbf{0}, \begin{bmatrix} k(\mathbf{X}_t, \mathbf{X}_t) + \sigma_n^2 I_{n \times n} & k(\mathbf{x}_{t+1}, \mathbf{X}_t) \\ k(\mathbf{X}_t, \mathbf{x}_{t+1}) & k(\mathbf{x}_{t+1}, \mathbf{x}_{t+1}) \end{bmatrix}\right) \quad (24)$$

where $\mathbf{y}_t = [y_1, \dots, y_t]$ and $\mathbf{X}_t = [\mathbf{x}_1, \dots, \mathbf{x}_t]$ is the state measurement vector. The predictive distribution $p(y_{t+1} | \mathbf{X}_t, y_t, \mathbf{x}_{t+1})$ from the above joint Gaussian prior distribution over the new input \mathbf{x}_{t+1} becomes [4]

$$\begin{aligned} p(y_{t+1} | \mathbf{X}_t, y_t, \mathbf{x}_{t+1}) &\sim \mathcal{N}(m_{t+1}, \Sigma_{t+1}) \\ m_{t+1} &= \alpha_{t+1}^T k(\mathbf{X}_{t+1}, \mathbf{x}_t) \\ \Sigma_{t+1} &= k(\mathbf{x}_{t+1}, \mathbf{x}_{t+1}) + k(\mathbf{X}_t, \mathbf{x}_{t+1})^T \mathbf{C}_t k(\mathbf{X}_t, \mathbf{x}_{t+1}) \\ \alpha_{t+1} &= \mathbf{C}_t \mathbf{y}_t \\ \mathbf{C}_t &= (k(\mathbf{X}_t, \mathbf{X}_t) + \sigma_n^2 I_{n \times n})^{-1} \end{aligned} \quad (25)$$

5.2 Sparse Gaussian Process Regression

Learning or regression problems that have fixed length of measurements have matrices with fixed cardinality and calculation of inverse operation for matrix costs fixed resources. On the other hand, online estimation problem has an increasing number of measurements, resulting in matrices whose size increases proportionally to the number of measurements. If GP regression is to be used on the online setting, it would be computationally intractable as the cardinality of the measurement set increases. So the number of the data points needs to be fixed for tractable calculation of the posterior mean. Csató and M. Opper proposed replacing data points, also known as basis vectors denoted \mathcal{BV} to maintain constant dataset size [4]. For addition and removal of the data points, the \mathcal{BV} must be re-evaluated with respect to the $t + 1$ datapoint. This can be done by kernel linear independence test [4], [3]. The linear independence test is as follows from [4], [3]

$$\gamma_{t+1} = \min_{\alpha_i} \left\| \sum_{i=1}^t \alpha_i k(\cdot, x_i) - k(\cdot, x_{t+1}) \right\|_{\mathcal{H}}^2 \quad (26)$$

whose solution α_t is also given as

$$\alpha_t = \mathbf{K}_{\mathbf{X}_t}^{-1} k(\mathbf{x}_{t+1}) \quad (27)$$

where $\mathbf{K}_{\mathbf{X}_t}$ is a gram matrix. The above equation leads to the following relationship of γ_{t+1} as

$$\gamma_{t+1} = k(\mathbf{x}_{t+1}, \mathbf{x}_{t+1}) - k(\mathbf{x}_{t+1}, \mathbf{x}_{t+1})^T \alpha_t \quad (28)$$

The above equation is used to check whether replacement of the new datapoint is required. When $\gamma_{t+1} > \beta_{tol}$ with user selected lower bound β_{tol} , it tells us that one of $\mathcal{B}\mathcal{V}$ needs replacement with new datapoint.

The proposed SGPR learning by Csató and M. Opper also calculates the parameters α_{t+1} and \mathbf{C}_{t+1} recursively [4]. For this to be done, when a data \mathbf{x}_{t+1} is observed at time $t+1$, the algorithm calculates following scalar variables are defined as,

$$\begin{aligned} q^{t+1} &= (y_{t+1} - \alpha_t^T \mathbf{k}_x) / \rho_s \\ r^{t+1} &= -\rho_s^{-1} \\ \rho_s &= \sigma_n^2 + k(\mathbf{x}_t, \mathbf{X}_t)^T \mathbf{C}_t k(\mathbf{x}_t, \mathbf{X}_t) + k(\mathbf{x}_t, \mathbf{x}_t) \end{aligned} \quad (29)$$

Then α_{t+1} and \mathbf{C}_{t+1} are calculated using the following recursive formulas

$$\begin{aligned} \alpha_{t+1} &= T_{t+1}(\alpha_t) + q^{t+1} \mathbf{s}_{s+1} \\ \mathbf{C}_{t+1} &= U_{t+1}(\mathbf{C}_t) + r^{t+1} \mathbf{s}_{s+1} \mathbf{s}_{s+1}^T \\ \mathbf{s}_{t+1} &= T_{t+1}(\mathbf{C}_t k_{\mathbf{x}_{t+1}}) + e_{t+1} \\ e_{t+1} &= \mathbf{Q}_t k(\mathbf{x}_{t+1}, \mathbf{X}_t) \\ \mathbf{Q}_t &= \mathbf{K}_{\mathbf{X}_t}^{-1} \end{aligned} \quad (30)$$

where $\mathbf{K}_{\mathbf{X}_t} = k(\mathbf{X}_t, \mathbf{X}_t)$. The $T_{t+1}(\cdot)$ and $U_{t+1}(\cdot)$ are operators to increase dimension of the $(t \times 1)$ vector and $(t \times t)$ matrix to $((t+1) \times 1)$ and $((t+1) \times (t+1))$ by concatenating zeros so that vector and matrix addition for increased dimension after adding or removing datapoint is possible. The size of the set $\mathcal{B}\mathcal{V}$ must be constant to make online regression possible. If adding datapoint from the previous recursive equation increases the dimension of the set $\mathcal{B}\mathcal{V}$, the least informative $\mathcal{B}\mathcal{V}$ must be removed. For this process, the scores are calculated using the following equation,

$$\varepsilon(i) = \frac{|\alpha_{t+1}(i)|}{\mathbf{Q}_{t+1}(i, i)} \quad (31)$$

The above equation is used to select the least informative $\mathcal{B}\mathcal{V}$ from the set. Define the least informative $\mathcal{B}\mathcal{V}$ index as i , then the following recursive equations update the parameters using set $\mathcal{B}\mathcal{V}$ with one data point removed.

$$\begin{aligned} \hat{\alpha}_{t+1} &= \alpha^r + \alpha(i) \frac{\mathbf{Q}(i)}{q(i)} \\ \hat{\mathbf{C}}_{t+1} &= \mathbf{C}^r + c(i) \frac{\mathbf{Q}(i) \mathbf{Q}(i)^T}{q(i)} - (\mathbf{Q}(i) \mathbf{C}(i)^T + \mathbf{C}(i) \mathbf{Q}(i)^T) \\ \hat{\mathbf{Q}}_{t+1} &= \mathbf{Q}^r - \frac{\mathbf{Q}(i) \mathbf{Q}(i)^T}{q(i)} \end{aligned} \quad (32)$$

In the above equation, the $\alpha(i)$, $c(i)$ and $q(i)$ are scalar variables from $\alpha_{t+1}(i)$, $\mathbf{C}_{t+1}(i, i)$ and $\mathbf{Q}_{t+1}(i, i)$. $\mathbf{C}(i)$ and $\mathbf{Q}(i)$ are $\mathbf{C}_{t+1}(:, i)$ and $\mathbf{Q}_{t+1}(:, i)$ vectors with i th component from each removed, hence their dimensions are $(t \times 1)$. The α^r is a vector α_{t+1} with $\alpha(i)$ component removed, also having $(t \times 1)$ dimension. In the same manner, \mathbf{C}^r and \mathbf{Q}^r are \mathbf{C}_{t+1} and \mathbf{Q}_{t+1} matrices with i th row and column removed having $(t \times t)$ dimensions.

Using SGPR, the uncertainties are estimated. The measurement y_t is obtained by the following equation

$$\begin{aligned}\hat{\alpha}_{t+1} &= \alpha^r + \alpha(i) \frac{\mathbf{Q}(i)}{q(i)} \\ \hat{\mathbf{C}}_{t+1} &= \mathbf{C}^r + c(i) \frac{\mathbf{Q}(i)\mathbf{Q}(i)^T}{q(i)} - (\mathbf{Q}(i)\mathbf{C}(i)^T + \mathbf{C}(i)\mathbf{Q}(i)^T) \\ \hat{\mathbf{Q}}_{t+1} &= \mathbf{Q}^r - \frac{\mathbf{Q}(i)\mathbf{Q}(i)^T}{q(i)}\end{aligned}\quad (33)$$

6. Simulation Result

The designed controller was used for controlling GTM with left main wing tip severed. The tip loss cases are 33 % and 40 %. The 40 % case was chosen to exaggerate differences between controllers used. To attain aerodynamic coefficients, CG shift, mass, and MOI, extrapolated values are used. The damage happens at 14 sec for both cases. The control variables are body rates. The figure 5 shows the result for NDI, INDI, and the proposed INDI SGPR of GTM that experiences 33 % left main wing tip loss. As the figure shows, the NDI controller failed to follow the reference command input. Among the other two controllers, the proposed INDI SGPR controller showed better reference command response, especially in the roll axis. The figure 6 shows the controllers response for 40 % left-wing damage case. The model-based NDI controller showed poor reference command following performance after damage occurred while the other two methods gave smaller errors. The INDI controller showed its robustness to uncertainties despite the damage though INDI with SGPR showed smaller error due to its adaptive term.

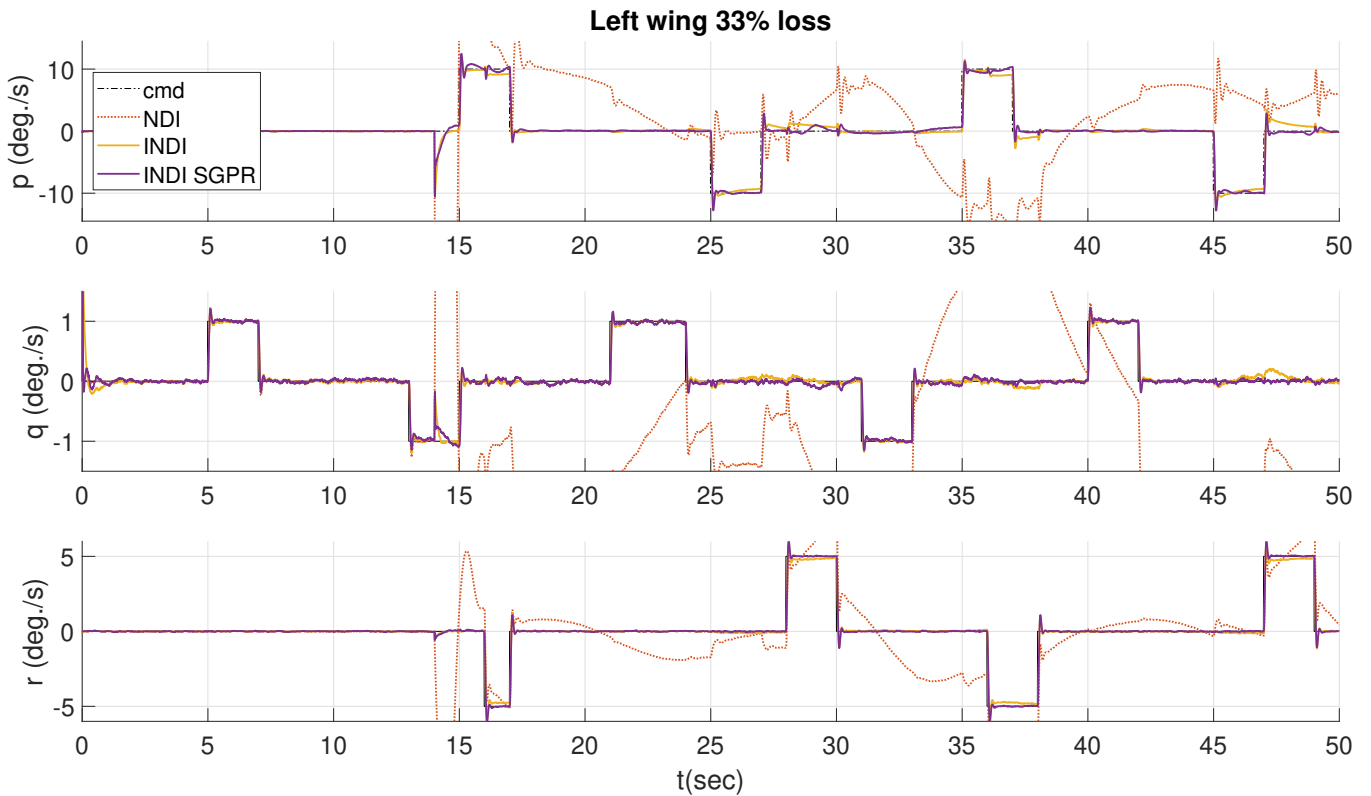


Figure 5 – NDI, INDI and INDI SGPR Control Response of p , q , and r for the GTM with 33 % severed left wing

7. Conclusion

A damaged fixed-wing aircraft control problem is being discussed. We proposed an INDI SGPR to attain robustness and adaptiveness. The aircraft model used is a ROM of GTM with 33 % loss of its left main wings. Changes in mass properties like mass, MOI, and CG shift are considered in the

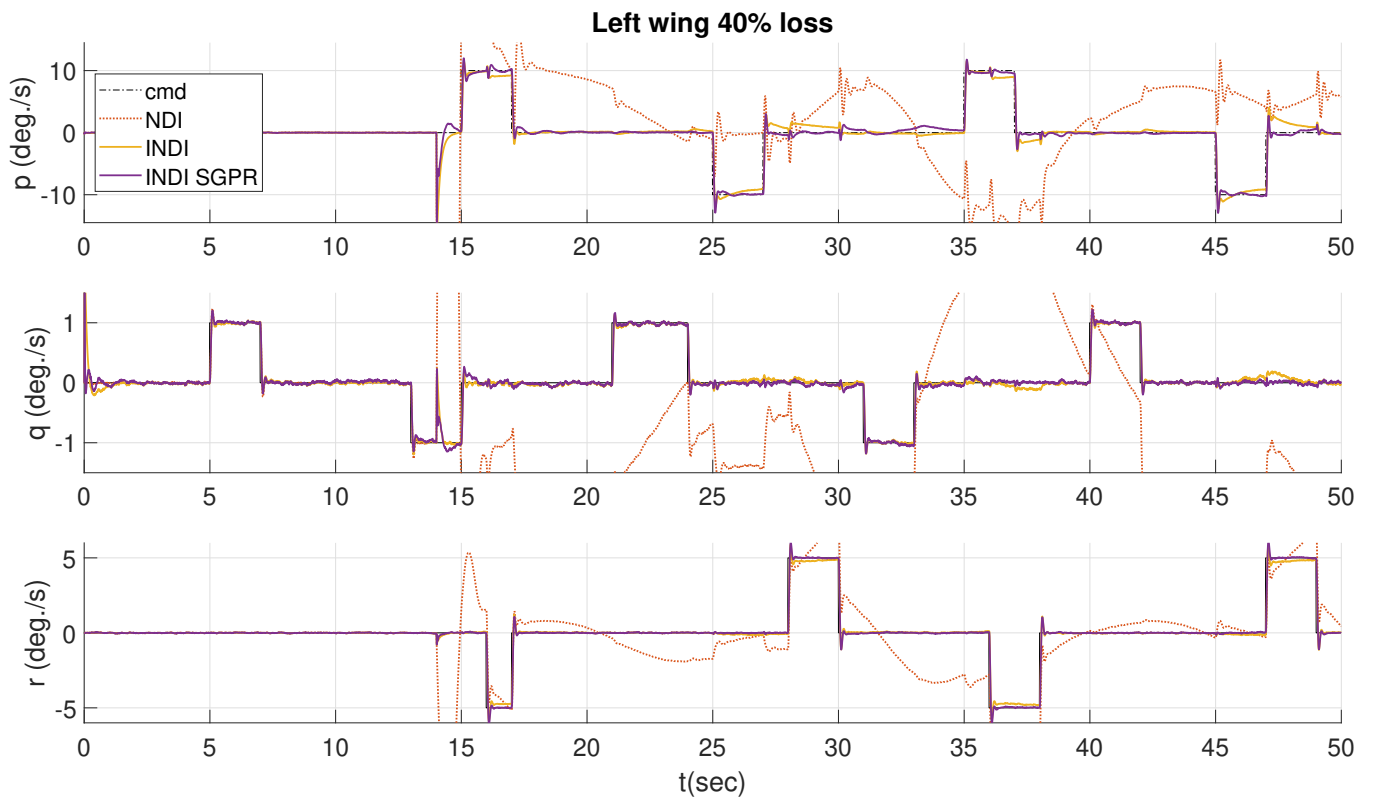


Figure 6 – NDI, INDI and INDI SGPR Control Response of p , q , and r for the GTM with 40% severed left wing

mathematical modeling together with the aerodynamic coefficient uncertainties due to damage. The proposed control sought to attain robustness by using incremental dynamics and adaptiveness by using SGPR which is a non-parametric Bayesian function sparse estimator. Three controllers are compared: NDI, INDI, and INDI SGPR. The simulation results showed that the proposed controller performed better than the other two controllers, especially on roll rate control.

8. Copyright Statement

The authors confirm that they, and/or their company or organization, hold copyright on all of the original material included in this paper. The authors also confirm that they have obtained permission, from the copyright holder of any third party material included in this paper, to publish it as part of their paper. The authors confirm that they give permission, or have obtained permission from the copyright holder of this paper, for the publication and distribution of this paper as part of the ICAS proceedings or as individual off-prints from the proceedings.

References

- [1] Barton Bacon and Irene Gregory. "General equations of motion for a damaged asymmetric aircraft". In: *AIAA atmospheric flight mechanics conference and exhibit*. 2007, p. 6306.
- [2] Gary Balas and John Hodgkinson. "Control design methods for good flying qualities". In: *AIAA Atmospheric Flight Mechanics Conference*. 2009, p. 6319.
- [3] Girish Chowdhary et al. "Bayesian nonparametric adaptive control using Gaussian processes". In: *IEEE transactions on neural networks and learning systems* 26.3 (2014), pp. 537–550.
- [4] Lehel Csató and Manfred Opper. "Sparse on-line Gaussian processes". In: *Neural computation* 14.3 (2002), pp. 641–668.
- [5] Mohamed K Helwa, Adam Heins, and Angela P Schoellig. "Provably robust learning-based approach for high-accuracy tracking control of lagrangian systems". In: *IEEE Robotics and Automation Letters* 4.2 (2019), pp. 1587–1594.

- [6] David Hughes and Michael A Dornheim. “DHL/EAT crew lands A300 with no hydraulics after being hit by missile”. In: *Aviation Week & Space Technology* 8 (2003).
- [7] Nhan Nguyen et al. “Dynamics and adaptive control for stability recovery of damaged asymmetric aircraft”. In: *AIAA Guidance, navigation, and control Conference and Exhibit*. 2006, p. 6049.
- [8] Ramin Norouzi. “Reconfiguring NASA Generic Transport Model for Normal Flight Envelope Simulation and Analysis”. In: *2018 9th International Conference on Mechanical and Aerospace Engineering (ICMAE)*. 2018, pp. 45–52. DOI: 10.1109/ICMAE.2018.8467651.
- [9] Jeffrey Ouellette et al. “Flight dynamics and structural load distribution for a damaged aircraft”. In: *AIAA atmospheric flight mechanics conference*. 2009, p. 6153.
- [10] Gautam Shah. “Aerodynamic effects and modeling of damage to transport aircraft”. In: *AIAA atmospheric flight mechanics conference and exhibit*. 2008, p. 6203.
- [11] RC van’t Veld. “Incremental Nonlinear Dynamic Inversion Flight Control: Stability and Robustness Analysis and Improvements”. In: (2016).
- [12] Xuerui Wang et al. “Stability analysis for incremental nonlinear dynamic inversion control”. In: *Journal of Guidance, Control, and Dynamics* 42.5 (2019), pp. 1116–1129.
- [13] Christopher KI Williams and Carl Edward Rasmussen. *Gaussian processes for machine learning*. Vol. 2. 3. MIT press Cambridge, MA, 2006.